Splitting electrons into quasiparticles with a fractional edge-state Mach-Zehnder interferometer

V. V. Ponomarenko
Center of Physics, University of Minho, Campus Gualtar, 47157 Braga, Portugal

D. V. Averin
Department of Physics and Astronomy, University of Stony Brook, SUNY, Stony Brook, New York 11794, USA

(Received 19 September 2008; revised manuscript received 29 November 2008; published 6 January 2009)

We have studied theoretically the tunneling between two edges of quantum Hall liquids of different filling factors, $\nu_{0,1}=1/(2m_{0,1}+1)$, with $m_0\geq m_1\geq 0$, through two separate point contacts in the geometry of Mach-Zehnder interferometer [Ji *et al.*, Nature (London) **422**, 415 (2003); Neder *et al.*, Phys. Rev. Lett. **96**, 016804 (2006)]. The quasiparticle formulation of the interferometer model is derived as a dual to the initial electron model in the limit of strong electron tunneling reached at large voltages or temperatures. For $m\equiv 1+m_0+m_1>1$, the tunneling of quasiparticles of fractional charge e/m leads to nontrivial m-state dynamics of effective flux through the interferometer, which restores the regular "electron" periodicity of the current in flux despite the fractional charge and statistics of quasiparticles. The exact solution available for equal times of propagation between the contacts along the two edges demonstrates that the interference pattern of modulation of the tunneling current by flux depends on voltage and temperature only through a common amplitude.

DOI: 10.1103/PhysRevB.79.045303 PACS number(s): 73.43.Jn, 71.10.Pm, 73.23.Ad

I. INTRODUCTION

Electronic Mach-Zehnder interferometers (MZIs) based on the integer quantum Hall states have been designed and studied in recent experiments.[1,2] This device consists of two tunneling contacts between two single-mode edges of the two-dimensional (2D) electron liquid in the regime of the integer quantum Hall effect, which are arranged to propagate effectively in the same direction. The interferometer enables one to observe pronounced interference patterns in the tunneling current. In anticipation of possible realization of similar interferometer based on the edges of electron liquids in the regime of the fractional quantum Hall effect (FQHE), MZI in this regime[3,4] and more complicated structures including it[5] were studied theoretically in search for signatures of the fractional statistics of FQHE quasiparticles. Some of these theories, however, (cf. Refs. 3 and 4) were based on different postulated models of the quasiparticle transport in MZI and obtained conflicting result, e.g., different periods of the tunnel current modulation by external magnetic flux Φ_{ex} through the interferometer.

In this work, whose main results have been briefly presented in Ref. 6, we consider tunneling between two edges of quantum Hall liquids (QHL) of in general different filling factors, $\nu_{0,1}=1/(2m_{0,1}+1)$ with $m_0\geq m_1\geq 0$, through two separate point contacts in the MZI geometry, and derive its quasiparticle model from the electronic description of the interferometer. The latter is always correct in the limit of weak tunneling, when the two edges are well separated from each other, and only whole electrons can be transferred between them through opaque tunnel barrier, which itself does not contain FQHE liquid. Using the scaling growth of electron-tunneling amplitudes with increasing voltage (or temperature), we demonstrate that the quasiparticle formulation of the interferometer model emerges naturally as a dual to the initial electron model in the limit of strong electron tunneling. This model shows that backscattering at the two interferometer contacts, which is weak for strong electron tunneling, produces quasiparticles of the same charge $e_X=2\nu_0\nu_1/(\nu_0+\nu_1)$ as in the situation of one point contact between the edges.[7] If the filling factors of the two edges are equal, the point-contact quasiparticles coincide[8] with the "bulk" Laughlin quasiparticles, as has been confirmed in the shot-noise experiments.[9]

The duality transformation used in this work to derive quasiparticles in the MZI, and the resulting quasiparticle tunnel Hamiltonian, are very similar to those in our previous treatment[10] of the antidot tunneling between fractional quantum Hall liquids (FQHLs) with different filling factors. Both systems exhibit an unusual phenomenon: Interference phase accumulated between the two point contacts is not determined solely by an external magnetic flux Φ_{ex} confined between the two edges but has a statistical contribution which transforms Φ_{ex} into an effective flux Φ. In the interferometer, each electron tunneling changes Φ by $\pm m\Phi_0$, where $m=1+m_0+m_1$ and $\Phi_0=2\pi\hbar c/e$ is a flux quantum equal to 2π in the units $(\hbar,c,e=1)$ we use in this paper, whereas in the case of the antidot tunneling, the similar factor m is given by $m=m_0-m_1$. (This difference reflects the difference in the edge propagation in the two structures. The two edges propagate in the same direction in the MZI, and in the opposite directions in the antidot.) As a result of this flux change, the system acquires m different quantum states, whose effective fluxes Φ differ from each other by $\Phi_0 \bmod m\Phi_0$. These states cannot be coupled by perturbative electron tunneling and therefore do not show up in the weak-tunneling "electron" regime. In the nonperturbative regime of strong tunneling, however, the states become mixed as Φ is changed by one flux quantum $\pm\Phi_0$ in the course of tunneling of individual quasiparticles. The charge transfer associated with this flux change, $e/m=e_X$, gives the fractional charge of the quasiparticles, which, in MZI, coincides with the usual point-contact quasiparticles in one point contact. In this respect, the MZI is different from the antidot formed by FQHLs with different filling factors, where the tunneling quasiparticles are different from those in one point contact, but can be

constructed from them through the process of multiple interference.[10] Our derivation of the quasiparticle Lagrangian in this work is a mathematical demonstration of such a splitting of electron into quasiparticles by the dynamics of flux. In the particular case of coincident filling factors, $\nu_0=\nu_1$, the model we derive agrees with the quasiparticle model assumed in Ref. 4. Our result also confirms that the quasiparticle model in Ref. 3 does not correspond to electron tunneling at two separate point contacts in the weak-tunneling limit, and probably does not represent any realizable geometry of an interferometer.

In the situation of symmetric interferometer, when the times t_0 and t_1 of propagation between the contacts along the two edges are equal $[\Delta t \equiv (t_0-t_1)/2=0]$, the quasiparticle Lagrangian can be solved by the methods of exactly solvable models. The resultant expression for the tunneling current can also be used for $V,T<1/\Delta t$. This exact expression describes the crossover from the regime of electron to quasiparticle tunneling with increasing voltages or temperatures. The tunneling conductance vanishes in both of the two limits of large and small voltages and/or temperatures. The large-voltage behavior of the exact tunneling conductance agrees to the leading order in large V with the conductance found in Ref. 4, limiting the validity of the quasiparticle calculation in Ref. 4 to this order. The conductance reaches its maximum of about $e^2/(2\pi\hbar m)$ in the crossover region between the regimes of electron and quasiparticle tunneling. The conductance peak extends between the energies defined by the bigger and the smaller of the two point-contact tunneling amplitudes, and therefore the peak width increases with increasing asymmetry between the two amplitudes. This asymmetry also makes the peak height larger, approaching more closely the saturation value $e^2/(2\pi\hbar m)$. In contrast to this, the magnitude of interference conductance oscillations as a function of the magnetic flux Φ_{ex} decreases steadily with increasing ratio of the two tunneling amplitudes. The oscillations should have the perfect 100% visibility in the interferometer with the identical point contacts.

The paper is organized as follows. Section II defines the electron-tunneling model considered in this work and presents perturbative calculation of the electron-tunneling current and integral visibility of its interference pattern in the regime of weak-electron tunneling. Section III treats the electron-tunneling model in the opposite limit of strong coupling in both contacts of the interferometer. We describe the bosonization procedure for the Klein factors of electron-tunneling operators which implements the flux attachment, and develop the instanton transformation leading to the dual model of quasiparticle tunneling. In the perturbative regime of weak quasiparticle tunneling, $V\Delta t \gg 1$ or $T\Delta t \gg 1$, we calculate the dc. Section IV presents perturbative calculations of the shot noise in both limits of weak-electron and weak-quasiparticle tunnelings. In Sec. V, we consider symmetric interferometer and obtain exact solution of its quasiparticle model, through fermionization for $m=2$ or by Bethe-ansatz technique for general m. This solution is used to calculate the average tunneling current in the interferometer and to analyze its dependence on the magnetic flux, voltage, and temperature.

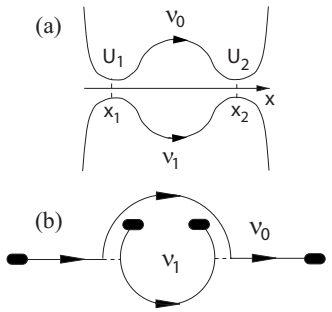

FIG. 1. Mach-Zehnder interferometer considered in this work. (a) Conceptual diagram of the two copropagating edges of QHLs with different filling factors ν_0 and ν_1 coupled at points x_j, $j=1,2$, by two point contacts with tunneling amplitudes U_j. The edges are assumed to support one bosonic mode each, with arrows indicating direction of propagation of these modes. (b) Schematic geometry of the edge propagation in the experimentally realized interferometers (Refs. 1 and 2). Filled areas denote the ohmic contacts which emit or absorb edge modes, and special arrangement of which makes it possible to implement tunneling between the copropagating edges within one plane of the two-dimensional electron gas.

II. ELECTRON-TUNNELING MODEL OF THE MACH-ZEHNDER INTERFEROMETER

A. Description of the edge states

To formulate the effective electronic model of the MZI (Fig. 1) we adopt the standard bosonization description of each of the two single-mode edges with filling factors $\nu_l=1/(2m_l+1)$, $l=0,1$. In this description, the electron operator ψ_l of the edge l is expressed as[11]

$$\psi_l = (D/2\pi v_l)^{1/2}\xi_l e^{i[\phi_l(x,t)/\sqrt{\nu_l}+k_l x]}.$$

Here ϕ_l are the two bosonic modes propagating in the same direction (in Fig. 1, to the right) with velocities v_l taken to be positive, $v_l>0$, the Majorana fermions ξ_l account for mutual statistics of electrons in different edges, and D is a common large-energy cutoff of the edge modes. The Fermi momenta k_l define the average electron density in the edges, while the operators of the density fluctuations are

$$\rho_l(x,\tau) = (\sqrt{\nu_l}/2\pi)\partial_x\phi_l(x,\tau).$$

The standard quadratic Lagrangian of the bosonic fields ϕ_l defines their real-time correlators, which at finite temperature T can be written as

$$\langle \phi_l(x,t)\phi_l(0,0)\rangle = -\ln\{\delta \sinh[\pi T(x/v_l - t + i/D)]\}, \quad (1)$$

where δ comes from an infrared cutoff and should be taken to zero at the end of calculations. Substituting this expression into the standard definitions of the retarded and/or advanced Green's functions $g^{R,A}(x,t)$ of these modes one finds

$$g^{R,A}(x,t) = \mp i\theta(\pm t)\langle[\phi_l(x,t),\phi_l]\rangle = \pm \pi\theta(\pm t)\mathrm{sgn}(x-v_l t). \quad (2)$$

The Fourier-transformed functions

$$g^{R,A}(x,\omega) = \int dt e^{i\omega t} g^{R,A}(x,t)$$

satisfy the condition $g^A(x,\omega)=[g^R(-x,\omega)]^*$ and are equal to

$$g^{R,A}(x,\omega) = \frac{2\pi}{i(\omega \pm i0)}\left(-\frac{\mathrm{sgn}(x)}{2} \pm \theta(\pm x)e^{i\omega x/v}\right).$$

Analytical continuation of these expressions according to the standard prescription $g(x,\omega)=-g^R(x,\omega)|_{\omega\to i\omega}$ for positive frequencies ω and $g(x,\omega)=-g^A(x,\omega)|_{\omega\to i\omega}$ for negative ω gives the Fourier transform of the imaginary-time-ordered correlators (see, e.g., Ref. 12),

$$\int_0^{1/T} d\tau e^{i\omega\tau}\langle T_\tau\{\phi_l(x,\tau)\phi_p(0,0)\}\rangle = \delta_{lp} g(x/v_l,\omega),$$

as follows:

$$g(z,\omega) = \frac{2\pi}{\omega}\mathrm{sgn}(z)\left(-\frac{1}{2} + \theta(\omega z)e^{-\omega z}\right). \quad (3)$$

The first term on the right-hand side of Eq. (3) defines the usual equal-time commutation relations,

$$[\phi_l(x),\phi_p(0)] = i\pi\,\mathrm{sgn}(x)\,\delta_{lp}.$$

B. Weak electron-tunneling model of MZI

With the bosonized electron operators, Lagrangian describing electron tunneling in the two contacts is

$$\mathcal{L}_t = \sum_{j=1,2}\left[\frac{DU_j}{2\pi}e^{i\kappa_j}e^{i\lambda\varphi_j} + \mathrm{H.c.}\right] \equiv \sum_{j=1,2}(T_j^+ + T_j^-), \quad (4)$$

where U_j and κ_j are the absolute values and the phases of the dimensionless tunneling amplitudes, and

$$\lambda\varphi_j(t) \equiv \frac{\phi_0(x_j,t)}{\sqrt{\nu_0}} - \frac{\phi_1(x_j,t)}{\sqrt{\nu_1}},$$

$$\lambda = \left[\frac{\nu_0+\nu_1}{\nu_0\nu_1}\right]^{1/2} = \sqrt{2m}. \quad (5)$$

The factor λ is chosen in such a way that the normalization of the bosonic operators φ_j coincides with that of the fields ϕ_l so that the imaginary-time correlators of φ_j are given by the same Eq. (3) with $z=0$: $g(0,\omega)=\pi/|\omega|$. The products of the Majorana fermions $\xi_1\xi_2$ were omitted from Lagrangian (4) since they cancel each other in each perturbative order due to charge conservation. The phases κ_j include contributions from the external magnetic flux Φ_{ex} through the interferometer and from the average numbers N_0 and N_1 of electrons accumulated, respectively, on the two sides of the interferometer between its tunnel contacts, so that

$$\kappa \equiv \kappa_2 - \kappa_1 = 2\pi[(\Phi_{ex}/\Phi_0) + (N_0/\nu_0) - (N_1/\nu_1)] + \mathrm{const}.$$

In practical devices,[1,2] the external magnetic flux Φ_{ex} is defined by the area enclosed between the propagating edges, including the area of the 2D electron gas of one of FQHLs [see Fig. 1(b)], which can be modified by a modulation gate. Note that nontrivial arrangement of the edges and tunneling contacts in practical devices shown in Fig. 1(b) is dictated by the confinement of the MZI structure to the plane of one 2D electron gas. In principle, more direct implementations of the electronic MZIs should be possible in the double-layer structures.

When a bias voltage V is applied to the interferometer, it creates a difference between the electrochemical potentials of the edges and also changes their local densities and hence the Fermi momenta. In the bosonic-field Lagrangian, the first effect can be accounted for by adding the time-dependent phase factors to the tunneling operators, $T_j(t)^\pm \to T_j^\pm(t)\exp\{\mp iVt\}$ in Eq. (4), while the second effect should change the phases κ_j. This means that the phase difference κ is also a function of the applied voltage V: $\kappa=\kappa(V)$. The voltage-induced contribution to κ depends on the electrostatics of the interferometer and on the way the voltage is applied. For instance, if the voltage changes the electrochemical potential of the edge 0 only, and the charge density is not fixed by electrostatics due to effective screening by an external gate, the phase varies as $\kappa(V)=\kappa+Vt_0$. If the voltage is applied to the edges symmetrically, then $\kappa(V)=\kappa+V(t_0+t_1)/2$. Moreover, if electron-tunneling amplitudes are not small, the current redistribution between the edges due to tunneling affects the average electron numbers $N_{0,1}$, and the interference phase κ in general should be determined self-consistently. On the other hand, if the charge density is fixed by electrostatics and voltage V cannot change the chemical potentials of the two edges, the phase difference should be independent of V: $\kappa(V)=\kappa$.

The operator of the electron tunnel current from the edge 0 into the edge 1 is found to have the usual form

$$I^e = i\left[\int dx\rho_0(x),\mathcal{H}\right] = \frac{\delta}{\delta\phi_0}\mathcal{L}_t = i\sum_{j=1,2}\sum_{\pm}(\pm)T_j^\pm e^{\mp iVt}.$$

Its average contains the phase-insensitive contribution $\bar{I}^e$ from the two point contacts independently, and the phase-sensitive interference term $\Delta I^e(\kappa)$

$$I = \langle I^e\rangle = \bar{I}^e + \Delta I^e(\kappa).$$

C. Perturbative calculation of electron-tunneling current

In the lowest nonvanishing order of the perturbation theory in U_j, the average tunneling current can be calculated as

$$I(V) = i\int_{-\infty}^0 dt\langle[I^e(0),\mathcal{L}_t(t)]\rangle$$

$$= \int_{-\infty}^{\infty} dt e^{iVt}\left\langle\left[\sum_j T_j^-(t),\sum_k T_k^+(0)\right]\right\rangle, \quad (6)$$

where the average $\langle\cdots\rangle$ is taken over the states of the two free propagating edges. Substituting the bosonic expression from Eq. (4), one finds the phase-insensitive term consisting of the two contributions from individual point contacts

$$\bar{I}^e = 2i\sum_j \left(\frac{DU_j}{2\pi}\right)^2 \int_{-\infty}^{\infty} dt e^{\lambda^2(\langle\varphi_j(t)\varphi_j(0)\rangle - \langle\varphi_j^2\rangle)} \sin Vt$$
$$= \sum_j (U_j^2 D/2\pi)(2\pi T/D)^{\lambda^2-1} C_{\lambda^2}(V/2\pi T), \quad (7)$$

where the second line follows[13] from Eq. (1) for the bosonic correlator, and

$$C_g(v) \equiv \sinh(\pi v)|\Gamma(g/2+iv)|^2/[\pi\Gamma(g)].$$

For g equal to an even positive number, this function reduces to the polynomial, $C_g(v)=v\Pi_{n=1}^{g/2-1}(n^2+v^2)/\Gamma(g)$.

The interference term can be written as

$$\Delta I^e = \left(\frac{U_1U_2D^2}{\pi^2}\right)\int_{-\infty}^{\infty} dt \,\mathrm{Im}\, e^{\lambda^2(\langle\varphi_2(t)\varphi_1(0)\rangle - \langle\varphi_1^2\rangle)} \sin[\kappa(V) - Vt]$$
$$= \left(\frac{U_1U_2D}{\pi^2}\right)\left(\frac{\pi T}{D}\right)^{\lambda^2-1} \int_{-\infty}^{\infty} ds \sin\left[\kappa(V) - V\bar{t} - \frac{sV}{\pi T}\right]$$
$$\times \mathrm{Im}\left\{\prod_{l=0,1}\{i\sinh[s-(-1)^l\Delta t\pi T - i0]^{-1/\nu_l}\}\right\} \quad (8)$$

in the notation $t_{0,1}=\bar{t}\pm\Delta t$. After redefinition of the phase, $\kappa_V=\kappa(V)-V\bar{t}$, Eq. (8) coincides with the interference term obtained in the antidot geometry.[10,14] Since the powers $1/\nu_l$ are integer, the integral in Eq. (8) can be transformed into a closed contour integral and evaluated by residues as follows:

$$\Delta I^e = \left(\frac{U_1U_2D^2}{\pi^2}\right)\left(\frac{\pi T}{iD}\right)^{\lambda^2} \sum_{m=0,1} \frac{\pi}{\Gamma(1/\nu_m)} \partial_s^{1/\nu_m-1} \left\{\frac{[s-(-1)^m\Delta t]^{1/\nu_m}\sin(sV-\kappa_V)}{\prod_{l=0,1}\{\sinh[(s-(-1)^l\Delta t)\pi T - i0]\}^{1/\nu_l}}\right\}\Bigg|_{s=(-1)^m\Delta t}. \quad (9)$$

At $T=0$, this expression describes an oscillating behavior of the phase-sensitive current. In the case $V\Delta t \gg 1$, it is characterized by the asymptotics

$$\Delta I^e \simeq \frac{2U_1U_2D\sin(V\Delta t)\cos(\kappa_V)(V/D)^{1/\nu-1}}{\pi i^{1/\nu+1}(1/\nu-1)!\,(2D\Delta t)^{1/\nu}}$$

for $\nu_0=\nu_1\equiv\nu$ and

$$\Delta I^e \simeq \frac{U_1U_2D\sin[Vt_0-\kappa(V)](V/D)^{1/\nu_0-1}}{\pi i^{1/\nu_1+1}(1/\nu_0-1)!\,(2D\Delta t)^{1/\nu_1}} \quad (10)$$

for $\nu_0\neq\nu_1$. The integral visibility of the interferometer is defined as

$$\mathrm{Vis} \equiv (\max_\kappa I - \min_\kappa I)/(\max_\kappa I + \min_\kappa I),$$

where the minimum and maximum are taken over the dependence of the current on the interference phase κ. Substituting the large-V asymptotics of current into this definition, one finds that for equal filling factors $\nu_0=\nu_1\equiv\nu$ the visibility decreases and oscillates with voltage as

$$\mathrm{Vis} \simeq \frac{(2/\nu-1)!}{(1/\nu-1)!}\frac{4U_1U_2}{U_1^2+U_2^2}\frac{|\sin(V\Delta t)|}{|2\Delta tV|^{1/\nu}}. \quad (11)$$

For $\nu=1$, this asymptotics becomes an exact expression for the integral visibility of integer quantum Hall MZI (Ref. 15) and was tested in experiments.[2] In this case, suppression of the interference is caused by linear variation in the interference phase with energy of propagating electrons. For $\nu_0<\nu_1$, the oscillations vanish asymptotically as

$$\mathrm{Vis} \simeq \frac{(\lambda^2-1)!}{(1/\nu_0-1)!}\frac{4U_1U_2}{U_1^2+U_2^2}|2\Delta tV|^{-1/\nu_1}. \quad (12)$$

Both expressions (11) and (12) generalize the description of the suppression of the interference due to variation in the phase of propagating excitations with energy from the case of integer edges to the edges with fractional filling factors.

In the opposite limit of $V,T<1/\Delta t$, the right-hand side of Eq. (9) sums up to the same polynomial $C_{\lambda^2}(V/2\pi T)$, and the full current $\langle I^e\rangle$ is given by Eq. (7) with the sum of squares of the two point-contact amplitudes U_j replaced by square of their coherent sum

$$I = \frac{|U_1+U_2e^{i\kappa_V}|^2D}{2\pi}(2\pi T/D)^{\lambda^2-1}C_{\lambda^2}(V/2\pi T). \quad (13)$$

In this regime, the visibility reaches its maximum

$$\mathrm{Vis} = 2U_1U_2/(U_1^2+U_2^2).$$

Appearance of the geometric sum of the two tunneling amplitudes in Eq. (13) suggests that for small Δt, the two-point-contact model of MZI described with Lagrangian (4) reduces to a single-point-contact model, but with the new amplitude. Indeed, such a single-point-contact model would provide an appropriate equivalent description of the two-point tunneling of noninteracting electrons, e.g., in a single-mode edge states in integer quantum Hall effect. Therefore, this reduction agrees with the usual practice[13] in studies of one-dimensional (1D) interacting electrons in quantum wires, where the two operations—the low-energy reduction in the multiple electron scattering to an effective single scatterer, and the switching on of the electron-electron interaction—are treated as interchangeable. However, the problem of FQHE edge states

transport is different. In particular, the dynamics of FQHE edge states is affected not by 1D but 2D electron interaction and geometry. We will show below that the interchange of the order of the operations is valid only in the lowest order in the limit of weak tunneling. In general, it would contradict the following physical feature of the system. Weak-electron-tunneling description (4) of the interferometer is intrinsically related to a strong-tunneling model. Indeed, as follows from Eq. (13), both of the amplitudes U_j scale at low energies E roughly as $E^{\lambda^2/2-1}$, where $E \simeq \max(V,T)$, and therefore increase with energy. The model of two FQHLs strongly coupled at two point contacts separated by a finite $\bar{t}$ possesses, however, a different topology than the single-point-contact model. Since the FQHL is a topological quantum liquid,[11] topology with two coupled points implies multiple degeneracy of the ground state, which leads, as will be seen more explicitly below, to the tunneling current different from that in the single-point contact.

III. STRONG-COUPLING LIMIT

A. Quantum nature of the effective magnetic flux

To derive the dual strong-coupling model for the MZI at large effective tunneling amplitudes U_j, we treat the problem in imaginary time and use the standard instanton technique. The ground states are determined by minimization of the action $\mathcal{S}$

$$\mathcal{S} = \mathcal{S}_{\rm kin} + \mathcal{S}_t, \tag{14}$$

which includes the tunneling part $\mathcal{S}_t$ defined by Lagrangian (4) and the kinetic term $\mathcal{S}_{\rm kin}$ defined by Eqs. (3) and (5). In the limit $U_j \gg 1$ for both $j=1,2$, tunneling Lagrangian (4) gives the dominant contribution to the action in Eq. (14). If the two parts of Lagrangian (4) that describe the two contacts were treated separately, both tunneling modes φ_j, $j=1,2$, would be fixed at the extrema of the corresponding parts of the Lagrangian. Considering both $T_j^{\pm}$ together, one can see, however, that their equal-time interchange relation is

$$T_2^{\pm} T_1^{\mp} = e^{2\pi m i} T_1^{\mp} T_2^{\pm}, \tag{15}$$

as follows from the commutation relation $[\varphi_2, \varphi_1] = i\pi$. As discussed in more detail below, this relation represents the essence of the MZI interference physics. It shows that although the different transfer terms $T_j^{\pm}$ [Eq. (4)] commute among themselves, each interchange of the electron-tunneling processes at the two contacts changes the interference phase κ so that the external magnetic flux $\Phi_{\rm ex}$ acquires an additional contribution $\pm m\Phi_0$. This mechanism transforms the external flux into effective flux Φ, which includes the statistical contribution, as discussed in Sec. I. While this statistical flux is irrelevant in the situation of weak-electron tunneling, it becomes crucial for the quasiparticle tunneling when effectively one needs to split the electron transfer terms with the associated exchange phase (15) into the transfer terms for the quasiparticles with fractional charge e/m. The corresponding splitting of the exchange phase into $2\pi/m$ terms is nontrivial.

B. Ground states and bosonization of Klein factors

The new statistical flux mechanism discussed above should affect the construction of the ground states of the interferometer in the strong-tunneling regime. To see how this happens, we first examine the perturbative expansion of the partition function in $U_{1,2}$. When imaginary times of two tunneling processes at different points, $T_1^{\pm}$ and $T_2^{\mp}$, change their time order, the phase branch of the perturbative term changes accordingly to Eq. (15). In general, one can make different choices for the phase branches by multiplying the tunneling operators $T_j^{\pm}$ with some Klein factors $\exp\{\pm i\sqrt{2\gamma}\eta_j\}$, where the free zero-energy bosonic modes η_j are defined by their imaginary-time-ordered correlators,

$$\langle T_\tau \eta_i(\tau)\eta_j(0)\rangle = i\pi\Theta[(j-i)\tau](1-\delta_{ij}). \tag{16}$$

For any integer γ, incorporation of these Klein factors into the terms $T_j^{\pm}$ in Eq. (4) does not change the perturbation expansion of the partition function in $\mathcal{S}_t$ in any order. Even integer γ affects, however, the kinetic part of the action. As we show below, this fact can be used to construct the ground states which minimize the energy of the system in the strong-coupling limit.

Indeed, the new tunneling fields Φ_j, which include the modes η_j

$$\Phi_j = \lambda\varphi_j + \sqrt{2\gamma}\eta_j,$$

are characterized by the kinetic action

$$\mathcal{S}_{\rm kin}[\gamma,(\Phi_{1,2})] = \int \frac{d\omega}{4\pi} \sum_{i,j} [\Phi_i(-\omega)\hat{K}_{ij}^{-1}(\gamma,\omega)\Phi_j(\omega)],$$

$$\hat{K}(\gamma,\omega) = \lambda^2 g(0,\omega)\hat{1} + \sum_{\pm}\left[\mp\frac{2\pi\gamma}{\omega} + \sum_j \frac{1}{\nu_j} g(\mp t_j,\omega)\right]\hat{\sigma}_{\pm}, \tag{17}$$

where $\hat{\sigma}_{\pm}$ are the raising and lowering 2×2 matrices, and the matrix $\hat{K}(\gamma)$ contains the correlators

$$K_{ij}(\gamma,\tau) = \lambda^2\langle T_\tau\varphi_i(\tau)\varphi_j(0)\rangle + 2\gamma\langle T_\tau\eta_i(\tau)\eta_j(0)\rangle.$$

Next, to construct the ground states, we follow the procedure from Ref. 16 and express the energy E_t associated with the electron-tunneling Lagrangian (4) in terms of the low-temperature asymptotics ($\beta \equiv 1/T \to \infty$) of the partition function of the system,

$$e^{-\beta E_t} = \frac{\int D\Phi e^{-\mathcal{S}(\gamma,\{\Phi_{1,2}\})}}{\int D\Phi e^{-\mathcal{S}_{\rm kin}(\gamma,\{\Phi_{1,2}\})}}. \tag{18}$$

Here the integrations $D\Phi \equiv \Pi_{j=1,2} D\Phi_j(\tau)$ run over functions defined on the imaginary-time interval $\tau \in [0,\beta]$ with the periodic boundary conditions. According to Eq. (14), the action $\mathcal{S}(\gamma,\{\Phi_{1,2}\})$ consists of the kinetic term $\mathcal{S}_{\rm kin}(\gamma,\{\Phi_{1,2}\})$ [Eq. (17)] and the tunneling part $\mathcal{S}_t$, which after substitution of the Klein factors takes the following form:

$$\mathcal{S}_t(\{\Phi_{1,2}\}) = -\int_0^\beta d\tau \sum_{j=1,2} \frac{DU_j}{\pi}\cos(\Phi_j + \kappa_j).$$

As discussed above, in the limit of small $U_{1,2}$, where the perturbative expansion in the electron transfer terms T_j is applicable, the energy E_t in Eq. (18) does not depend on γ. However, in the strong-coupling limit of large U's, the dominant tunneling part of the action $\mathcal{S}$ imposes the strong-tunneling conditions

$$\Phi_j = 2\pi n_j - \kappa_j \equiv \Phi_{n_j} \quad \text{for } j = 1,2, \tag{19}$$

in the upper functional integral in Eq. (18). As a result, the energy E_t, which can be expressed as

$$E_t = \int \frac{d\omega}{4\pi}\ln[\mathrm{Det}\,\hat{K}(\gamma,\omega)]e^{-|\omega|/D} + \frac{\mathcal{S}(\gamma,\{\Phi_{n_j}\})}{\beta}, \tag{20}$$

acquires dependence on the parameter γ. Substitution of the matrix $\hat{K}(\gamma)$ from Eq. (17) into Eq. (20) gives the γ-dependent part of E_t as

$$E_t = \int \frac{d\omega}{4\pi}\ln\left[m^2 + (\gamma - m)^2 + (\gamma - m)\sum_j \frac{e^{-|\omega|t_j}}{\nu_j}\right]e^{-|\omega|/D} + \frac{\delta_{\gamma,0}(n_1 - n_2 + \kappa)^2}{\sum_j (t_j/\nu_j)} + \text{const}.$$

Minimization of this expression at $t_{0,1}D \gg 1$ imposes unambiguously the choice $\gamma = m$, which also guarantees commutativity of the two tunneling fields Φ_j. The commutativity is important to make the strong-tunneling conditions [Eq. (19)] self-consistent. On the other hand, in the limit $t_{0,1}D \to 0$, the minimum of E_t occurs for $\gamma = 0$. This is precisely the limit when we can be sure that the tunneling at the two point contacts reduces to a single-point tunneling characterized by the effective amplitude equal to the geometrical sum of the two point-contact amplitudes.

Next, we discuss briefly how the incorporation of the chosen bosonic Klein factors into the full tunneling operators $T_{Cj}^{\pm} \equiv T_j^{\pm}\exp\{\pm i\sqrt{2m}\eta_j\}$ affects our earlier interpretation of the physics underlying Eq. (15). Qualitatively, the Klein factors change the dynamics of interchange relations [Eq. (15)]. Indeed, one can see directly that the phase factor of Eq. (15) drops out from the equal-time interchange relation of the full tunneling operators T_{Cj}. It, however, reappears when their time difference is much larger than both propagation times $t_{0,1}$. In particular, we find that for $\tau \gg t_{0,1}$

$$(T_{C2}^- T_{C1}^+)(0)T_{C1,2}^+(-\tau) = e^{-2\pi m i}T_{C1,2}^+(\tau)(T_{C2}^- T_{C1}^+)(0). \tag{21}$$

This new relation characterizes dynamics of the mechanism of the effective flux transformation we discussed above: Each process of electron tunneling in any of the two contacts of the interferometer modifies the interference pattern for subsequent electrons passing through the interferometer at much later times, as if the effective flux is changed by $m\Phi_0$.

C. Instanton expansion and duality transformation

The standard instanton calculation of the partition function $\mathcal{Z}$ for infinitely degenerate series (19) of the ground states (Φ_{n_1}, Φ_{n_2}) leads us to the expression $\mathcal{Z} = \Sigma_{n_j}\mathcal{Z}_{n_1,n_2}$. Each term in this sum is calculated through the substitution into $\exp\{-\mathcal{S}(\Phi_1,\Phi_2)\}$ of the asymptotic form of the instanton expansion around the (Φ_{n_1}, Φ_{n_2}) ground state

$$\Phi_j(\tau) = \Phi_{n_j} + \sum_l 2\pi e_{l,j}\theta(\tau - \tau_{l,j}),$$

and further summation over the number of instantons $e_{l,j} = 1$ and anti-instantons $e_{l,j} = -1$, and integration over their times $\tau_{l,j}$. The result can be presented in the following form:

$$\mathcal{Z}_{n_1,n_2} \propto \int D\Theta_{1,2}\exp\left\{-\mathcal{S}_{\mathrm{kin}}^D + \sum_j \frac{W_j D}{2\pi}\int d\tau\cos[\Theta_j(\tau) + (-1)^j(\kappa_j - 2\pi n_j)/m]\right\} \tag{22}$$

with a constant of proportionality independent of $n_{1,2}$. The new kinetic term in this action is defined as

$$\mathcal{S}_{\mathrm{kin}}^D(\Theta) = \frac{1}{2}\int \frac{d\omega}{2\pi}\Theta(-\omega)[(2\pi/\omega)^2\hat{K}^{-1}(\omega)]^{-1}\Theta(\omega),$$

$$\left(\frac{2\pi}{\omega}\right)^2\hat{K}^{-1} = \frac{4\pi}{\lambda^2|\omega|}\hat{1} + \sum_{\pm,j} \pm\frac{8\pi}{\lambda^4\omega}\frac{e^{\pm\omega t_j}}{\nu_j}\theta(\mp\omega)\hat{\sigma}_{\pm} \tag{23}$$

by instanton-instanton interaction, while the phases of cosines in Eq. (22) follow from the interaction between instantons and the $n_{1,2}$ ground state.

Comparing the correlators of the fields Θ defined by this action to $g(z,\omega)$ in Eq. (3), we can divide these fields into the two parts

$$\Theta_j = (-1)^j\left[\sqrt{\frac{2}{m}}\eta_j + \frac{2}{\lambda}\vartheta_j\right]. \tag{24}$$

The bosonic modes $\eta_{1,2}$ describe here purely statistical effect (16), while the fields ϑ have the chiral correlators

$$\langle\vartheta_j^2\rangle = g(0,\omega), \langle\vartheta_2\vartheta_1\rangle = \frac{g(t_0,\omega)}{\nu_0\lambda^2} + \frac{g(t_1,\omega)}{\nu_1\lambda^2}. \tag{25}$$

Notice further that the contribution $\mathcal{Z}_{n_1,n_2}$ in Eq. (22) depends on both n_1 and n_2 only through their difference mod m. Therefore, up to a divergent constant, $\mathcal{Z}$ becomes a finite sum. This sum over the indices combined with integration of the exponents of the re-extracted statistical fields can be represented as a trace over the m-dimensional Hilbert space. This is achieved by ascribing to each instanton tunneling exponent in Eq. (22) a proper m-dimensional matrix. These unitary matrices $\bar{F}_j$ are characterized by the following relations:

$$\bar{F}_1\bar{F}_2 = e^{-2\pi i/m}\bar{F}_2\bar{F}_1, \quad \langle\bar{F}_1^k(\bar{F}_1^+)^p\bar{F}_2^l(\bar{F}_2^+)^q\rangle = \delta_{kp}\delta_{lq}, \tag{26}$$

where the Kronecker symbol δ_{ij} is defined mod m. The first relation in Eq. (26) is due to the statistical parts of the fields

Θ in Eq. (24), while the second one follows from the m-periodic dependence of Eq. (22) on both indices. Writing $\mathcal{Z}$ in the form of the trace makes it equal to a partition function of the quasiparticles whose tunneling Lagrangian $\bar{\mathcal{L}}_t$ in real time has the form dual to Lagrangian (4),

$$\bar{\mathcal{L}}_t = \sum_{j=1,2}\left[\frac{W_j D}{2\pi}\bar{F}_j \exp\left\{i\left(\frac{\kappa_j(V)}{m}+\frac{2\vartheta_j}{\lambda}-\frac{Vt}{m}\right)\right\}+\text{H.c.}\right]$$
$$\equiv \sum_{j=1,2}\sum_{\pm}\bar{T}_j^{\pm}e^{\mp iVt/m}. \tag{27}$$

The operators $\bar{F}_j$ here are the Klein factors describing the statistics of the quasiparticles. These factors are analogous to the Klein factors derived in Ref. 10 for the quasiparticle tunneling in the antidot geometry. They act in the Hilbert space spanned by the m-fold degenerate ground state of the MZI in the absence of the quasiparticle tunneling. As discussed in Sec. I, in both the antidot and the MZI geometries, the m states correspond to different effective flux Φ enclosed by the edges between the two point contacts. The quasiparticle model of the MZI based on tunnel Lagrangian (27) derived above generalizes the quasiparticle model in Ref. 4, which used a particular form of the matrix Klein factors complying with Eq. (26) up to a phase factor we find below.

Finally, using quasiparticle expression (32) for the tunneling current that is obtained in Sec. III D, we proceed to the perturbative calculation of this current,

$$I(V) = i\int_{-\infty}^{0} dt\langle[I^q(0),\bar{\mathcal{L}}_t(t)]\rangle$$
$$= \frac{1}{m}\int_{-\infty}^{\infty} dt e^{iVt/m}\left\langle\left[\sum_j \bar{T}_j^-(t),\sum_l \bar{T}_l^+(0)\right]\right\rangle. \tag{28}$$

It should be noted that the average in this expression includes, in particular, the average over the m-dimensional Hilbert space of the flux states taken according to Eq. (26). This makes the interference term vanish in the lowest perturbative order, the fact that suggests suppression of the interference in general in model (27) of the quasiparticle tunneling. In our discussion of the electron-tunneling model in Sec. II, we saw, however, that the interference is suppressed only if $V\Delta t \gg 1$ or $T\Delta t \gg 1$. As will be shown below, the same is true in the regime of the quasiparticle tunneling. Validity of perturbative result (28) which predicts suppressed interference is indeed restricted to the regimes of $V\Delta t \gg 1$ or $T\Delta t \gg 1$. For $(V,T)\Delta t < 1$, solution of Lagrangian (27) is nonperturbative.

D. Boundary conditions, dual chiral fields, and edge currents

To clarify the dynamics of the tunneling fields ϑ_j defined by Eq. (24) and to explain the introduction of the applied voltage in Eq. (27), we need to relate the tunneling fields ϑ_j to the incoming edge modes $\phi_{0,1}$. To do this, we first consider the case of $\Delta t=0$ and equal velocities of the edge modes ϕ_l. In this case, both tunneling bosonic operators φ_j in Eq. (4) are just the two operator values of the same bosonic field ϕ_- at points $x_{1,2}$: $\varphi_j=\phi_-(x_j)$, where in the absence of tunneling, the field

$$\phi_- = \frac{\sqrt{\nu_1}\phi_0 - \sqrt{\nu_0}\phi_1}{\sqrt{\nu_0+\nu_1}} \tag{29}$$

is a free chiral filed. The combination ϕ_+ of the two edge modes that is orthogonal to ϕ_-,

$$\phi_+ = \frac{\sqrt{\nu_0}\phi_0 + \sqrt{\nu_1}\phi_1}{\sqrt{\nu_0+\nu_1}}, \tag{30}$$

is not affected by tunneling at all and is always a free chiral field. In the strong-coupling limit of the two tunneling terms,

$$\mathcal{L}_{t,j} = (DU_j/\pi)\cos[\lambda\phi_-(x_j)+\kappa_j]$$

treated independently of each other, the propagation of ϕ_- is described by imposing the Dirichlet boundary condition. "Unfolded" form of this condition[17] implies free chiral propagation of the fields $\text{sgn}(x-x_j)[\phi_-(x)+\kappa_j/\lambda]$ across each point contact x_j. Application of these boundary conditions at both contacts successively implies that the field outgoing from the first contact is used as the incoming filed for the second contact. This procedure results in the free propagation of the chiral field that can be written for all values of x as

$$\vartheta_-(x) = \phi_-(x)\theta(x_1-x)+\left(\phi_-(x)-2\frac{\kappa}{\lambda}\right)\theta(x-x_2)$$
$$-\left(\phi_-(x)+2\frac{\kappa_1}{\lambda}\right)\theta(x-x_1)\theta(x_2-x). \tag{31}$$

This strong-coupling propagation of $\phi_-(x)$ implies that it changes sign and acquires some phase shifts on both passages through x_j. Finite quasiparticle backscattering leads to deviations from free chiral propagation (31) and is described by the dual tunneling terms $\bar{\mathcal{L}}_{t,j}=(DW_j/\pi)\cos\{(2/\lambda)[\phi_-(x_j)+\kappa_j/\lambda]\}$. Expressed through the free chiral dual field ϑ_- [Eq. (31)], these dual tunneling terms take the form

$$\bar{\mathcal{L}}_{t,j} = (DW_j/\pi)\cos\{(2/\lambda)[\vartheta_-(x_j)+\kappa_j/\lambda]\}.$$

Their comparison with the tunneling Lagrangian in Eq. (27) derived by the instanton expansion shows that the tunneling fields ϑ_j in Eq. (27) are related to the dual chiral field as $\vartheta_j=\vartheta_-(x_j)$ in agreement with Eq. (25). Both parts $\Sigma_{\pm}\bar{T}_{1,2}^{\pm}$ of tunneling Lagrangian (27) are constructed from the dual tunneling fields which are combined with the Klein factors to restore the commutativity.

To understand how the applied voltage V enters in Eq. (27), we note that the applied voltage can be introduced at first as a shift of the incoming field: $\phi_0-\sqrt{\nu_0}Vt$. As one can see from Eqs. (29) and (31), this shift translates into the shift $\vartheta_- - Vt/\lambda$ of the dual field, producing the voltage bias in the quasiparticle Lagrangian shown in Eq. (27). Also, since at the end of its propagation through the MZI, the ϕ_- field again coincides with ϑ_- field (27) up to a constant, the tunneling current in the MZI is produced only by the deviations of the ϑ_- field from its free propagation that are caused by the dual tunneling terms. Relating variations in ϕ_0 to variations in ϕ_- through Eqs. (29) and (30), one finds the quasiparticle tunneling current to be equal to

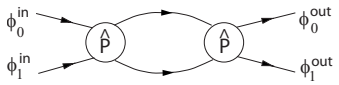

FIG. 2. Diagram of the strong-coupling edge propagation in the Mach-Zehnder interferometer.

$$I^q = \frac{i}{\lambda}\left[\bar{\mathcal{L}}_t, \int \frac{dx}{2\pi}\partial_x \vartheta_-(x)\right] = \frac{i}{m}\sum_{j=1,2}\sum_{\pm} \pm \bar{T}_j^{\pm} e^{\mp iVt/m}. \tag{32}$$

Both of these results, for the bias voltage and for the tunneling current, can be understood simply as manifestations of the fractional charge e/m of the quasiparticles.

The picture of successive splitting of the edges at the two point contacts in the strong-coupling regime that underlies Eq. (31) remains valid for $\Delta t \neq 0$, with the edge fractions propagating along the two sides of the interferometer remaining the same as those that follow from Eqs. (29)–(31). This means that the whole picture of propagation of charges and currents carried by the ϕ_j fields in the MZI can be represented in general with the diagram shown in Fig. 2, where each of the matrices $\hat{P}$ is[7,12]

$$P_{00} = -P_{11} = \frac{\nu_0 - \nu_1}{\nu_0 + \nu_1}, \quad P_{01} = P_{10} = -\frac{2\sqrt{\nu_0\nu_1}}{\nu_0 + \nu_1}, \tag{33}$$

and describes the edge splitting at the point contact. Matrix (33) satisfies the identity $\hat{\mathbf{P}}^2 = \hat{1}$, which implies that the two consecutive scattering processes at the point contacts do not change the current distribution between the modes of the interferometer. For instance, in the case of equal filling factors, $\nu_0 = \nu_1$, the matrix $\hat{\mathbf{P}}$ just interchanges the edge modes in both contacts. Therefore, the tunneling current in the MZI is created only by the dual tunneling terms, and Eq. (32) for this current is valid independently of Δt.

Besides transferring fractional charge of quasiparticles e/m, each dual tunneling also changes the effective flux through the MZI. This can be seen explicitly from the relation

$$(\bar{T}_2^- \bar{T}_1^+)(0)\bar{F}_{1,2}(-\tau) = e^{-2\pi i/m}\bar{F}_{1,2}(\tau)(\bar{T}_2^- \bar{T}_1^+)(0), \tag{34}$$

which follows from Eq. (26). For $\tau \gg t_{0,1}$, the bosonic exponents of the tunneling operators do not affect this interchange relation. Equation (34) is analogous to Eq. (21) for electrons, and characterizes dynamics of the effective flux transformation: Each tunneling of a quasiparticle in any of the two interferometer contacts adds flux quantum Φ_0 to the effective flux through the interferometer, which modifies the interference phase for quasiparticles tunneling much later through the interferometer. In this respect, interchange relations (34) agree with the physical picture suggested in Refs. 4 and 5 and derived earlier in the context of the antidot tunneling,[10] in which each tunneling quasiparticle also carries with it a flux quantum. An important unresolved question of this picture is to what extent the statistical contribution to the interference phase can be understood directly as a real change in the magnetic flux through the interferometer.

The simplest m-dimensional irreducible representation for the Klein factors that account for this flux changes is

$$X_{l,j} = \delta_{l+1,j} (\mathrm{mod}\ m), \quad Y_{l,j} = \delta_{l,j} e^{-i(2\pi/m)l}.$$

If we apply a unitary transformation, it takes a flux-diagonal form

$$\bar{F}_1 = X, \bar{F}_2 = -e^{\pm i\pi/m} XY.$$

The phase factor here follows from the second equation in Eq. (26). In the case $m=2$, these Klein factors are equal to the Pauli matrices: $\bar{F}_{1,2} = \sigma_{X,Y}$.

IV. SHOT NOISE OF THE TUNNELING CURRENT

In general, the noise power spectrum of the current I^a at frequency ω and voltage V, where $a = e, q$ denotes, respectively, the electron or quasiparticle form of the tunneling current, is defined as

$$P(\omega, V) = \int_{-\infty}^{\infty} dt\, \cos(\omega t)(\langle I^a(t) I^a(0)\rangle - \langle I^a\rangle^2).$$

In the lowest-order perturbation theory in the respective tunneling amplitudes, this expression takes form

$$P(\omega, V) = q_a^2 \int_{-\infty}^{\infty} dt\, \cos(\omega t) e^{iVtq_a} \times \left\langle \left\{ \sum_j T_j^{a-}(t), \sum_l T_l^{a+}(0) \right\} \right\rangle. \tag{35}$$

Here q_a is the charge of the tunneling particles which is equal to 1 or $1/m$ in units of the electron charge e, and $T^{a\pm}$ stands for $T^{\pm}$ or $\bar{T}^{\pm}$ in the regime of, respectively, electron and quasiparticle tunneling. Comparison of Eq. (35) with perturbative expressions for the tunneling current in Eqs. (6) and (28) shows immediately that the average currents and the noise power spectra are related in the lowest order of the perturbation theory as

$$P(\omega, V) = \frac{q_a}{2}\sum_{\pm} \coth[(q_a V \pm \omega)/(2T)] I(q_a V \pm \omega). \tag{36}$$

On the other hand, the zero-frequency limit of the noise power and the average current can be found from the long-time asymptotics of the distribution of the tunneling charge as its second and first moment divided by time. At $T=0$, and in the lowest order in the tunneling amplitudes, this distribution corresponds to a Poisson process, and therefore the Schottky formula for the shot noise $P(0,V)/I(V) = q_a$ displays directly the charge of the tunneling particles. This charge is e at low voltages, and e/m at sufficiently large voltages, if $V\Delta t > 1$ and the perturbative treatment of the quasiparticle tunneling model is correct. It is important to stress here that although the fractional charge e/m coincides with the charge e_X of the point-contact quasiparticles in the situation of tunneling in one point contact,[7] it appears in Eq. (36) for the quasiparticle noise in the MZI by a purely statistical mechanism. This mechanism is the reduction in the

MZI flux variations from $\pm m\Phi_0$, which are produced by electron tunneling in accordance with the composite-fermion statistics of electrons in both edges, to $\pm\Phi_0$ associated with the quasiparticle tunneling. This interpretation of the statistical origin of the fractional charge in Eq. (36) is supported also by the analysis[10] of the antidot interferometer, where the two charges are different, $e/m \neq e_X$, and e/m is the charge in the noise spectrum.

V. EXACT SOLUTION FOR SYMMETRIC MZI MODEL

A. Fermionization for $\nu_0=1/3$ and $\nu_1=1$

We now return to the case of symmetric interferometer with $\Delta t=0$, and consider derived dual model (27) in the case $\lambda=2$ (i.e., for $\nu_0=1/3$ and $\nu_1=1$), when the main parts, $e^{\pm i\vartheta_-}$, of the quasiparticle tunneling operators have the same correlators as free electrons, and therefore allow fermionization. Indeed, the Klein factors for $m=2$ can be represented by two Pauli matrices and fermionized as $\bar{F}_j=i\xi_j\xi_0$ in terms of the three Majorana fermions $\{\xi_n,\xi_{n'}\}_+=2\delta_{n,n'}$. Introducing a chiral fermion field as

$$\psi=\xi_0\sqrt{D/(2\pi v)}e^{i\vartheta_-},$$

we come to the Hamiltonian

$$\mathcal{H}=\left\{\frac{v}{i}\int dx\psi^+\partial_x\psi\right\} - \sqrt{\frac{Dv}{2\pi}}\left[\sum_j W_j i\xi_j\psi(x_j)e^{(i/2)\kappa_{j,V}}+\text{H.c.}\right], \quad (37)$$

where the applied voltage is accounted for by the fermion chemical potential equal to $V/2$. In fermionic Hamiltonian (37), the two terms accounting for successive tunneling at x_1 and x_2 contain two different Majorana fermions, the fact that distinguishes this Hamiltonian from the fermionic Hamiltonian in Ref. 3. As a result, the Heisenberg equations of motion which describe scattering of the field $\psi(x,t)$ at the two point contacts have the form of the *disentangled* matching conditions

$$i\psi(x)|_{x_j-0}^{x_j+0}=w_j\xi_j, \quad w_j\equiv i\sqrt{D/(2\pi v)}W_j e^{-(i/2)\kappa_{jV}},$$

$$\partial_t\xi_j(t)=2iv[w_j\psi^+(x_j,t)-w_j^*\psi(x_j,t)]. \quad (38)$$

Free chiral propagation of the field $\psi(x,t)$ everywhere else (away from the point contacts x_1 and x_2) makes it convenient to formulate scattering conditions [Eq. (38)] in terms of chiral momentum eigenstates of the Fourier components ψ_k of the free chiral field,

$$\psi_0(x,t)=\int\frac{dk}{2\pi}\psi_k e^{ik(x-vt)},$$

since this field coincides with the field $\psi(x,t)$ in the absence of scattering. Conditions [Eq. (38)] then mix together the components ψ_k and ψ_{-k}^+, which have the same time dependence and can be interpreted as annihilation operators of particle and hole states, respectively. Solution of Eq. (38) for scattering at each of the two point contacts shows that the evolution of the amplitudes of ψ_k and ψ_{-k}^+ across this contact can be described explicitly by the (2×2) scattering matrix $\hat{\mathcal{S}}_{j,k}$ with the elements

$$\mathcal{S}_{j,k}^{\pm\pm}=\frac{k}{k+i2|w_j|^2}, \quad \mathcal{S}_{j,k}^{-+}=\frac{2iw_j^2}{k+i2|w_j|^2}=\mathcal{S}_{j,-k}^{+-*}. \quad (39)$$

Successive scattering of the particles and holes at the two-point contacts is governed then by the scattering matrix $\hat{\mathcal{S}}_k$ equal to the product $\hat{\mathcal{S}}_k=\hat{\mathcal{S}}_{2,k}\hat{\mathcal{S}}_{1,k}$ of the scattering matrices at the two contacts. The particles incident on the point contacts have the fermi distribution $f(k,\mu)$ over the momenta k with the chemical potential $\mu=q_aV$, where the quasiparticle charge is $q_a=1/2$ in units of electron charge e. Summing the scattering processes for particles with different momenta and using the standard properties of the scattering matrix,

$$1-|S_k^{++}|^2=|S_k^{-+}|^2,$$

we can express the average tunneling current in terms of this matrix as follows:

$$I=\frac{1}{2}\int\frac{dk}{2\pi}[f(k,V/2)-f(k,-V/2)]|S_k^{-+}|^2 = \int\frac{dk}{2\pi}[f(k,V/2)-f(k,0)]\frac{\left|2ik\sum_j w_j^2\right|^2}{\prod_j|(k+2i|w_j|^2)|^2}. \quad (40)$$

Splitting the product over $j=1,2$ in Eq. (40) into a difference of two fractions, and introducing the tunneling rates $\Gamma_j\equiv 2v|w_j|^2=DW_j^2/\pi$, one can see that current (40) can be expressed as the difference between the tunneling currents in two individual point contacts,

$$I=\frac{|\Gamma_1 e^{i\kappa_V}+\Gamma_2|^2}{\Gamma_1^2-\Gamma_2^2}[I_{1/2}(V,\Gamma_2)-I_{1/2}(V,\Gamma_1)]. \quad (41)$$

The tunneling current in a separate point contact is known to be equal to[13]

$$I_{1/2}(V,\Gamma)=\frac{\sigma_0}{2}[V-2\Gamma\ \arctan(V/2\Gamma)]$$

at vanishing temperature T and to[18]

$$I_{1/2}(V,\Gamma)=\frac{\sigma_0}{2}\left[V-2\Gamma\ \text{Im}\ \psi\left(\frac{1}{2}+\frac{2\Gamma+iV}{2\pi T}\right)\right] \quad (42)$$

at nonzero T. Here $\psi(z)=d\ln\Gamma(z)/dz$ is the digamma function, and $\sigma_0=e^2/2\pi\hbar$ is the conductance quantum equal to $1/2\pi$ in the units $(e=\hbar=1)$ used in this paper.

At $T=0$, the low-voltage asymptotics of the tunneling current I in the MZI is proportional to V^3 and coincides with the electron-tunneling current in Eq. (13) under the condition $U_j=\pi W_j^{-2}/2$, which is expected from the single-point-contact duality as discussed below [see Eqs. (52) and (53)]. At large voltages, the current saturates at the constant value

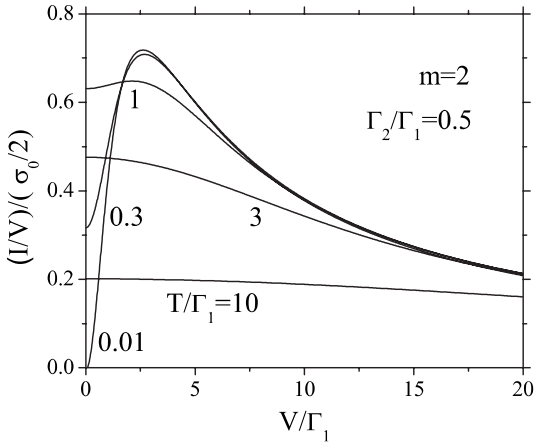

FIG. 3. Tunneling conductance of the symmetric Mach-Zehnder interferometer formed between the edges with filling factors $\nu_0=1/3$ and $\nu_1=1$ as a function of the bias voltage V between them for several temperatures T in the case of maximum constructive interference, $\kappa_V=0$. The conductance is calculated from Eqs. (41) and (42). The curves illustrate the low-T crossover between the electron-tunneling regime at low voltages and tunneling of the edge-state quasiparticles of charge $e/2$ at large voltages. The crossover is manifested in the conductance peak at the intermediate voltages which disappears with increasing temperature.

$$I=\frac{\pi\sigma_0}{2}\frac{|\Gamma_1 e^{i\kappa_V}+\Gamma_2|^2}{\Gamma_1+\Gamma_2}. \tag{43}$$

At nonvanishing temperatures, the current I depends linearly on voltage V at $V\ll T$. The corresponding linear conductance is suppressed at large temperatures $T\gg\Gamma_{1,2}$ as

$$G=\frac{\pi\sigma_0}{4T}\frac{|\Gamma_1 e^{i\kappa_V}+\Gamma_2|^2}{\Gamma_1+\Gamma_2}. \tag{44}$$

Behavior of the tunnel conductance $G\equiv I/V$ of the interferometer at arbitrary temperatures is illustrated in Fig. 3, which plots the conductance based on Eqs. (41) and (42) in the case of constructive interference, $\kappa_V=0$. Note that for $\Delta t=0$ as assumed in this section, the conductance G depends on the interference phase κ_V only through the amplitude $|\Gamma_1 e^{i\kappa_V}+\Gamma_2|$, which gives the full 100% modulation of G for identical contacts, when $\Gamma_1=\Gamma_2$, and suppression of the modulation with increasing contact asymmetry. At $T\to 0$, the conductance reflects the crossover from the regime of electron tunneling at small voltages, characterized by $G\propto V^2$, to the regime of quasiparticle tunneling at large voltages, where $G\propto 1/V$. The conductance reaches maximum in the crossover region. The rate of electron tunneling is enhanced by nonvanishing temperatures so that $G\propto T^2$, when $V\ll T\ll\Gamma_{1,2}$. At large temperatures, $T>\Gamma_{1,2}$, the electron-tunneling regime effectively disappears, and conductance approaches asymptotic value (44) that is independent of the voltage V in the range $V<T$.

We note that the results for the current I obtained above do not depend on the average propagation time $\bar{t}$ between the contacts, and are symmetric with respect to the interchange of the contact indices 1 and 2. It is therefore instructive to consider the limit $x_1=x_2$, when Eq. (38) is transformed into

$$\partial_t\xi_j(t)=2iv[w_j\psi^+(x_j,t)-w_j^*\psi(x_j,t)],$$

$$i\psi(x)|_{x_1-0}^{x_1+0}=\sum_j w_j\xi_j. \tag{45}$$

Substitution into these equations of the operators $\psi(x,t)$ and $\xi_{1,2}(t)$ in the following form,

$$\psi(x,t)=\int\frac{dk}{2\pi}e^{ik(x-vt)}[\theta(x_1-x)\psi_k+\theta(x-x_1)(S_k^{++}\psi_k+S_k^{-+}\psi_{-k}^+)],$$

$$\xi_j(t)=\int\frac{dk}{2\pi}e^{ik(x-vt)}\xi_{j,k}, \tag{46}$$

shows that

$$S_k^{-+}=\frac{2ik\sum_j w_j^2}{\left(k+i\sum_j|w_j|^2\right)^2+\left|\sum_j w_j^2\right|^2}. \tag{47}$$

Making use of this S-matrix element in the first part of Eq. (40), we find the expression for the current which can be cast in the form similar to Eq. (41),

$$I=\frac{\Gamma_+-\Gamma_-}{\Gamma_++\Gamma_-}[I_{1/2}(V,\Gamma_-)-I_{1/2}(V,\Gamma_+)], \tag{48}$$

where $\Gamma_\pm=v(\Sigma_j|w_j|^2\pm|\Sigma_j w_j^2|)$. In general, $\Gamma_\pm$ differ from $\Gamma_{1,2}$ so that the two current-voltage characteristics for two different point contacts and for one "combined" contact do not coincide. This shows that although current (41) is independent of the propagation time $\bar{t}$, it does depend on the fact that $\bar{t}$ is nonvanishing. Nevertheless, since $\Gamma_++\Gamma_-=\Gamma_1+\Gamma_2$ and $\Gamma_+-\Gamma_-=|\Gamma_1 e^{i\kappa_V}+\Gamma_2|$, the two current-voltage characteristics have the same large-voltage [Eq. (43)] and large-temperature [Eq. (44)] behavior. This large-energy equality is "symmetric" to the fact that low-energy asymptotics [Eq. (13)] of the electron tunnel current for negligible Δt is given by the single-contact expression with the geometric sum of the electron-tunneling amplitudes.

B. Bethe-ansatz solution

The results for $\lambda=2$ discussed above can be generalized to other values of $\lambda^2=2m$, for which a thermodynamic Bethe-ansatz solution is known[19] for a single-point tunneling contact. The solution exploits a set of quasiparticle states describing local $\vartheta_-(x)$ excitations and introduced through the massless limit of the sine-Gordon model. These quasiparticles are kinks, antikinks, and breathers of the height defined by the sine-Gordon interaction and equal to $\pi\lambda$. They remain interacting in the massless limit as described by a bulk S matrix, but undergo separate one-by-one scattering at the point contact described by a one-particle boundary S matrix.[20] Their scattering at the two point contacts occurs successively and independently at different points, as follows

from the dynamics of the local fluctuations of the field $\vartheta_-(x)$ derived above through application of the "unfolded" Dirichlet boundary conditions. Therefore, the overall scattering is described by the product of the two boundary S matrices dependent on the phases κ_1 and κ_2, respectively. To obtain these matrices from the one found in Ref. 19 in the case of $\kappa=0$, we notice that each phase κ_j in Eq. (27) results from the shift of ϑ_- by the constant κ_j/λ. Hence, the operators $\exp(\pm i\lambda\vartheta_-/2)$ of the ϑ_- kinks and/or antikinks acquire just constant phase factors $e^{\pm i\kappa_j/2}$. The boundary S matrix in Ref. 19 transforms then into

$$\mathcal{S}_{j,k}^{\pm\pm}=\frac{(ak/T_{jB})^{m-1}e^{i\alpha_k}}{1+i(ak/T_{jB})^{m-1}},\quad \mathcal{S}_{j,k}^{-+}=\frac{e^{i(\alpha_k-\kappa_{jV})}}{1+i(ak/T_{jB})^{m-1}},\quad (49)$$

where the dimensional factor

$$a=v\frac{2\sqrt{\pi}\Gamma\{1/[2(1-\nu)]\}}{\nu\Gamma\{\nu/[2(1-\nu)]\}}$$

redefining the energy scales T_{jB} is added into Eq. (49) to simplify the formulas below. The tunneling current produced by the kink-antikink transitions breaking the charge conservation takes the following form for the two-point contact:

$$I=\int_0^\infty v\,dk|(\hat{\mathcal{S}}_2\hat{\mathcal{S}}_1)^{-,+}|^2 n[f_+-f_-].\quad (50)$$

Notice that both the density of states $n(k,V)$ and the distribution functions $f_\pm$ for kinks and antikinks, are defined by the "bulk" of the system and do not depend on the scattering at the point contacts. This means that the tunneling current in Eq. (50) takes the form that generalizes Eq. (41)

$$\frac{I}{V}=\frac{|T_{1B}^{m-1}e^{i\kappa_V}+T_{2B}^{m-1}|^2}{T_{1B}^{2(m-1)}-T_{2B}^{2(m-1)}}[G_{1/m}(V/T_{2B},T/T_{2B})-G_{1/m}(V/T_{1B},T/T_{1B})],\quad (51)$$

where $G_{1/m}(V/T_{jB},T/T_{jB})$ is the universal scaling function of the tunneling conductance of a single-point contact between the two effective edges of the filling factor $\nu=1/m$. This function has been found[19] from the Bethe-ansatz solution, and at zero temperature reduces to the low- and high-voltage expansion series

$$G_\nu(s,0)=\sigma_0\nu\sum_{n=1}^{\infty}c_n\left(\frac{1}{\nu}\right)s^{2n(1/\nu-1)}\quad \text{for}\quad s<e^\Delta,$$

$$G_\nu(s,0)=\sigma_0\nu\left[1-\sum_{n=1}^{\infty}c_n(\nu)s^{2n(\nu-1)}\right]\quad \text{for}\quad s>e^\Delta,$$

$$c_n(\nu)=(-1)^{n+1}\frac{\Gamma(\nu n+1)\Gamma(3/2)}{\Gamma(n+1)\Gamma[3/2+(\nu-1)n]},$$

where

$$e^\Delta=(\sqrt{\nu})^{\nu/(1-\nu)}\sqrt{1-\nu}.$$

Substitution of these expansions into Eq. (51) gives the low-voltage asymptotics of the tunneling current for $V<T_{jB}e^\Delta$ as

$$\frac{I}{V}=\frac{\sigma_0}{m}c_1(m)V^{2(m-1)}\left|\sum_{j=1}^{2}T_{jB}^{1-m}e^{i\kappa_{jV}}\right|^2,$$

and its large-voltage asymptotics for $V>T_{jB}e^\Delta$ as

$$\frac{I}{V}=\frac{\sigma_0}{m}c_1\left(\frac{1}{m}\right)V^{2/m-2}\left|\sum_{j=1}^{2}T_{jB}^{m-1}e^{-i\kappa_{jV}}\right|^2\frac{T_{1B}^{2-2/m}-T_{2B}^{2-2/m}}{T_{1B}^{2(m-1)}-T_{2B}^{2(m-1)}}.$$

The energy scales T_{jB} are related to both correspondent electron and quasiparticle tunneling amplitudes U_j, W_j in the same way

$$T_{jB}=2D\left(\frac{U_j}{\Gamma(1/\nu)}\right)^{-[\nu/(1-\nu)]},\quad (52)$$

$$T_{jB}=\frac{2}{\nu}D\left(\frac{W_j}{\Gamma(\nu)}\right)^{1/(1-\nu)},\quad (53)$$

as in the case of the individual point contact.[21] Substitution of Eq. (52) into the low-voltage asymptotics reproduces exactly perturbative electron-tunneling current (13) upon application of the identity $\sqrt{\pi}\Gamma(2m)=2^{2m-1}\Gamma(m)\Gamma(m+1/2)$. On the other hand, making use of Eq. (53) one can rewrite the large-voltage asymptotics in terms of the quasiparticle tunneling amplitudes

$$\frac{I}{V}=\frac{\left|\sum_{j=1}^{2}W_j^m e^{-i\kappa_{jV}}\right|^2}{2\pi\Gamma(2/m)}\frac{W_1^2-W_2^2}{W_1^{2m}-W_2^{2m}}\left(\frac{V}{mD}\right)^{(2/m)-2},$$

which agrees in the leading order with the calculation in Ref. 4. Although the tunneling conductance vanishes as a negative power of voltage (and temperature), it always remains nonperturbative in the quasiparticle tunneling amplitudes. This nonperturbative dependence is a consequence of the inherent resonance condition $|V\Delta t|<1$ in the exact solution. Notice that the nonperturbative behavior of the MZI takes place at large energies contrary to the case of the antidot interferometer,[10] where the resonant condition also leads to a nonperturbative behavior, but at low energies. This difference is related to formation of resonances around the antidot, which cannot be formed in the MZI, where the two edges propagate in the same direction.

Several other general features follow directly from expression (51) for the current. Equation (51) shows that the current interference has the same dependence on both V and T as the function $G_{1/m}$ of the single-point tunneling conductance. This similarity holds only when $V\Delta t, T\Delta t\ll 1$. Indeed, as we have seen from Eq. (9), in the perturbative regime of electron tunneling, the condition $V\Delta t\gg 1$ leads to the power-law suppression of the interference current, and this suppression should become exponential for $T\Delta t\gg 1$. Equation (51) also shows that, similarly to Eq. (13), the visibility of the interference pattern does not vary with temperature and voltage as long as $V\Delta t, T\Delta t\ll 1$. In this regime, the interference pattern produced by the dependence of the current on the external magnetic flux has the same form of the simple one-mode modulation and is not affected by the change from electron to quasiparticle tunneling.

To further clarify the typical patterns of the current modulation by the interference phase κ_V, we consider Eq. (51) in the two limits: $T_{2B} \ll T_{1B}$ and $T_{2B}=T_{1B}$. In the first case, expression for the tunneling conductance simplifies to

$$G \simeq \left[1 + 2\cos\kappa_V \left(\frac{T_{2B}}{T_{1B}}\right)^{m-1}\right][G_{1/m}(V/T_{2B}, T/T_{2B}) - G_{1/m}(V/T_{1B}, T/T_{1B})], \quad (54)$$

which shows that for $T_{2B} < (T \text{ or } V) < T_{1B}$, the conductance exhibits weak oscillations of the amplitude $U_1/U_2 = (W_2/W_1)^m$ as a function of the external magnetic flux close to the single-point-contact saturation value σ_0/m. For $V, T < T_{2B}$, or if at least one of the energies is larger than T_{1B}, the conductance goes to zero. Although the proportionality of the amplitude of the interference oscillations to the mth power, W_2^m, of the smaller quasiparticle tunneling amplitude has entered Eq. (54) through single-point-contact duality relations (52) and (53) between U_2 and W_2, one can also interpret it as a manifestation of the quasiparticle statistics. Indeed, in the general quasiparticle tunneling model described by Lagrangian (27), the appearance of W_2^m in the amplitude of the current oscillations is a mathematical consequence of Klein factor relations [Eq. (25)]. In terms of physics, it is also necessary in order to restore the Φ_0 periodicity of the current in the external magnetic flux since the quasiparticle statistics implies that each tunneling of a quasiparticle changes the effective flux for other quasiparticles by Φ_0/m. Therefore, in the MZI, the W_2^m dependence of the current oscillation amplitude and the appearance of e/m fractional charge in the quasiparticle shot noise discussed earlier both originate from the fractional statistics of the quasiparticles.

In the case of identical contacts $T_{2B}=T_{1B}$ and for $T=0$, Eq. (51) can be written as

$$G = \frac{2\cos^2(\kappa_V/2)}{m-1} V \partial_V G_{1/m}\left(\frac{V}{T_B}\right). \quad (55)$$

Its average over the magnetic-flux oscillations is equal to the oscillation amplitude, and also coincides[22] with the doubled shot noise $2\langle I^2\rangle(V,T_B)/V$ of the tunneling current through the point contact divided by the voltage. At finite temperature T, the linear conductance is also given by Eq. (55) with the voltage V replaced by temperature T.

The zero-temperature tunneling conductance at the intermediate ratios T_{2B}/T_{1B} calculated from Eq. (51) for $m=3$ is plotted in Fig. 4. The conductance is shown in the case of maximum constructive interference, $\kappa_V=0$. As discussed above, the conductance depends on the interference phase κ_V only through the prefactor $|T_{1B}^{m-1}e^{i\kappa_V}+T_{2B}^{m-1}|$ so that the magnitude of the interference current decreases monotonically with the degree of asymmetry between the two contacts. Figure 4 shows that the width of the crossover region between the electron tunneling at low voltages and quasiparticle tunneling at large voltages increases with increasing contact asymmetry. Simultaneously with the increasing width of the conductance peak in the crossover region, its height increases toward the conductance saturation value σ_0/m. This behavior is consistent with the simple qualitative picture of the total tunneling current being the difference between currents in the two point contacts. The larger the difference between the two energy scales T_{1B} and T_{2B}, the larger is the voltage region where the conductance of the more transparent contact already reached the saturation, while the conductance of the less transparent contact remains small.

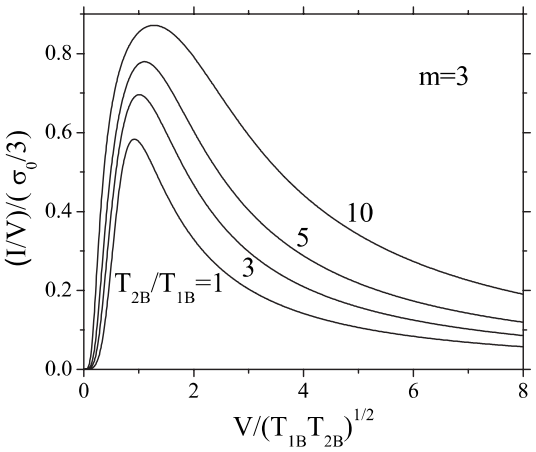

FIG. 4. Zero-temperature tunneling conductance (51) of the symmetric Mach-Zehnder interferometer with $m=3$ (formed, e.g., between the two edges with filling factors $\nu_0=1/3$) as a function of the bias voltage V for different degrees of the asymmetry between the two interferometer contacts in the case of maximum constructive interference, $\kappa_V=0$. The curves illustrate the crossover between the electron tunneling at low voltages and quasiparticles tunneling at large voltages. The crossover region is seen as the conductance peak between the two regimes.

VI. SUMMARY AND DISCUSSION

Starting from the electron-tunneling model of the electronic Mach-Zehnder interferometer that is natural at low voltages and/or temperatures, when the tunneling is weak, we have calculated the quantum average of current at all energies. The average current oscillates as a function of magnetic flux with the period of one flux quantum due to interference of tunneling electrons at low energies and quasiparticles at high energies. The low-energy calculation shows that the interference oscillations are suppressed with increasing difference Δt of the propagation times along the two edges, due to variations in the interference phases with energy and/or momentum of the propagating excitations. The tunneling current does not depend on the average propagation time $\bar{t}$, and for $\Delta t=0$, in the lowest order of the perturbation theory in the electron-tunneling amplitudes, does not distinguish the geometrically different situations of $\bar{t}=0$ and $\bar{t}\neq 0$.

Description of the strong-tunneling regime, which emerges with increasing voltages and/or temperatures, has been obtained by employing the instanton duality transformation that introduces the quasiparticle tunneling between the infinitely degenerate ground states of the interferometer. The ground states are defined by a choice of the branch of the phase produced by interchange of electron-tunneling processes at the two point contacts. This phase gives the statis-

tical variation in the effective magnetic flux through the interferometer. By minimizing the tunneling energy, we have found the phase equal to $2\pi m$ at $(t_0+t_1)D \gg 1$, and derived the model [Eqs. (25)–(27)] of the quasiparticle tunneling in the Mach-Zehnder interferometer for arbitrary filling factors of the interferometer edges. Although the tunneling terms at both contacts have vanishing scaling dimension at high energies, the perturbative treatment of the model at these energies is possible only if $\Delta t V \gg 1$ or $\Delta t T \gg 1$, and the interference between the two tunneling operators is suppressed. In this regime, the fractional charge of the tunneling quasiparticles manifests itself in the Schottky formula for the shot noise.

In the opposite limit of symmetric interferometer, $\Delta t=0$, the model remains nonperturbative at high energies, but allows the general exact solution which describes the crossover from electron to quasiparticle tunneling. The interference pattern of the current is characterized by the single-harmonic modulation, which is the same in both tunneling regimes, and is independent of the voltage and temperature. The modulation amplitude of the average current and also the current shot noise carry signatures of the fractional statistics of the quasiparticles.

It is interesting to compare our main exact result (51) for the tunneling current with the solution one would obtain by taking the zero-phase branch in the interchange relations of the tunneling terms, which follows from the minimization of energy at $(t_0+t_1)D \ll 1$. In this situation, the geometry does not prevent us from combining the two tunneling contacts together into one effective point contact with the tunneling amplitude $U_1+U_2e^{i\kappa_V}$. Its tunneling current can then be found by substitution of this amplitude into Eq. (52) and the expressions for $G_{1/m}$. It has the following low-energy expansion:

$$\frac{I}{V} = \frac{1}{2\pi}\sum_{n=1}^{\infty} \frac{c_n(m)}{m}\left(\frac{|U_1 + U_2 e^{i\kappa_V}|}{\Gamma(m)}\right)^{2n}\left(\frac{V}{2D}\right)^{2n(m-1)}.$$

This expansion differs from the low-energy expansion of current (51) already in the second lowest order in the tunneling amplitudes. In this order, it involves two oscillating harmonics as a function of κ_V. This means that already the next order in the perturbative expansion (discussed in Sec. II C) for the electron-tunneling current should distinguish the geometry with $\bar{t}=0$ from the geometry with $\bar{t}\neq 0$. Even more noticeably, the difference in the geometry of the tunneling contact would lead to the different limiting values of the tunneling conductance at large energies.

ACKNOWLEDGMENTS

V.V.P. would like to thank Alvaro Ferraz for hospitality and useful discussions during his stay at the International Center for Condensed Matter Physics at the University of Brasilia in Brazil, where a part of this work was done. V.V.P. also acknowledges support of the MCT of Brazil during this stay, of the ESF Science Program INSTANS under the Grant No. PTDC/FIS/64926/2006.

[1] Y. Ji, Y. C. Chung, D. Sprinzak, M. Heiblum, D. Mahalu, and H. Shtrikman, Nature (London) **422**, 415 (2003); I. Neder, M. Heiblum, Y. Levinson, D. Mahalu, and V. Umansky, Phys. Rev. Lett. **96**, 016804 (2006).
[2] L. V. Litvin, H.-P. Tranitz, W. Wegscheider, and C. Strunk, Phys. Rev. B **75**, 033315 (2007).
[3] T. Jonckheere, P. Devillard, A. Crepieux, and T. Martin, Phys. Rev. B **72**, 201305(R) (2005).
[4] K. T. Law, D. E. Feldman, and Y. Gefen, Phys. Rev. B **74**, 045319 (2006).
[5] C. L. Kane, Phys. Rev. Lett. **90**, 226802 (2003).
[6] V. V. Ponomarenko and D. V. Averin, Phys. Rev. Lett. **99**, 066803 (2007).
[7] C. C. Chamon and E. Fradkin, Phys. Rev. B **56**, 2012 (1997); N. P. Sandler, C. C. Chamon, and E. Fradkin, *ibid.* **57**, 12324 (1998); **59**, 12521 (1999).
[8] C. L. Kane and M. P. A. Fisher, Phys. Rev. Lett. **72**, 724 (1994).
[9] R. de Picciotto, M. Reznikov, M. Heiblum, V. Umansky, G. Bunin, and D. Mahalu, Nature (London) **389**, 162 (1997); L. Saminadayar, D. C. Glattli, Y. Jin, and B. Etienne, Phys. Rev. Lett. **79**, 2526 (1997).
[10] V. V. Ponomarenko and D. V. Averin, Phys. Rev. B **71**, 241308(R) (2005).
[11] X. G. Wen, Adv. Phys. **44**, 405 (1995).
[12] V. V. Ponomarenko and D. V. Averin, Phys. Rev. B **70**, 195316 (2004).
[13] C. L. Kane and M. P. A. Fisher, Phys. Rev. B **46**, 15233 (1992).
[14] M. R. Geller and D. Loss, Phys. Rev. B **56**, 9692 (1997).
[15] V. S.-W. Chung, P. Samuelsson, and M. Buttiker, Phys. Rev. B **72**, 125320 (2005).
[16] V. V. Ponomarenko and D. V. Averin, Phys. Rev. B **67**, 035314 (2003); JETP Lett. **74**, 87 (2001).
[17] Ch. Nayak, M. P. A. Fisher, A. W. W. Ludwig, and H. H. Lin, Phys. Rev. B **59**, 15694 (1999).
[18] U. Weiss, M. Sassetti, Th. Negele, and M. Wollensak, Z. Phys. B: Condens. Matter **84**, 471 (1991).
[19] P. Fendley, A. W. W. Ludwig, and H. Saleur, Phys. Rev. Lett. **74**, 3005 (1995); Phys. Rev. B **52**, 8934 (1995).
[20] S. Ghosshal and A. B. Zamolodchikov, Int. J. Mod. Phys. A **9**, 3841 (1994).
[21] U. Weiss, Solid State Commun. **100**, 281 (1996).
[22] P. Fendley, A. W. W. Ludwig, and H. Saleur, Phys. Rev. Lett. **75**, 2196 (1995).